A simple 3-D constitutive model for both clay and sand
黏土和砂土简单的三维本构模型

YAO Yang-ping(姚仰平)[1], LUO Ting(罗 汀)[1], SUN De-an(孙德安)[2], MATSUOKA Hajime(松冈元)[2]
(1. Department of Civil Engineering, Beijing University of Aeronautics and Astronaustics, Beijing 100083, China; 2. Department of Civil Engineering, Nagoya Institute of Technology, Nagoya 466-8555, Japan)

Abstract: A simple and unified constitutive model for both clay and sand under three-dimensional stress conditions is derived from the modified Cam-clay model, taking the following two points into consideration. First, a transformed stress tensor based on the SMP (Spatially Mobilized Plane) criterion is applied to the Cam-clay model. The proposed model realizes the consistency from the shear yield to the shear failure and the combination of the idea of the critical state theory with the SMP criterion for clay. Secondly, a new hardening parameter is derived in order to develop a simple and unified constitutive model for both clay and sand. It can not only describe the dilatancy from lightly to heavily dilatant sand, but also be reduced to the plastic volumetric strain for clay. The validity of the hardening parameter is confirmed by the test results of triaxial compression and extension tests on sand under the various stress paths. Only five conventional soil parameters are needed in the proposed model.

Key words: clays; sands; elasto-plastic model; hardening parameter; three-dimensional stresses
CLC number: TU 432 Document code: A Article ID: 1000-4548(2002)02-0240-07
Biography: YAO Yang-ping(1960-), male, Xi'an, shanxi, professor, Ph. D. major research topics: soil elastoplastic model, soil dynamics.

摘 要: 把修正剑桥模型推广为适合于黏土和砂土的简单、统一三维本构模型是基于以下两点提出的: 第一点, 把由笔者已提出的基于SMP准则的一个变换应力张量用于修正剑桥模型使其简单实现了三维化, 改进的模型对于黏土实现了从剪切屈服到剪切破坏的统一及临界状态理论同SMP准则的结合; 第二点, 为了建立对于黏土和砂土简单、统一的本构模型, 推导出了一个新的硬化参数, 新硬化参数不仅能描述砂土不同程度的剪胀性, 对于正常固结黏土又能退化成塑性体积应变, 所提硬化参数的合理性也被各种路径下分别在三轴压缩和三轴伸长下的试验结果所证实。所提模型的计算参数仅为5个常规试验参数, 易于确定。

关键词: 黏土; 砂土; 弹塑性模型; 硬化参数; 三维化

1 Introduction*

The modified Cam-clay model, which is suitable for clay (in this paper, the term clay is to be interpreted as the normally consolidated clay), was proposed by Roscoe and Burland[1]. The modified Cam-clay model and many other models have been generalized by assuming a section of the yield surface to be circular in the π-plane. That is to say, the criterion of the Extended Mises type (q/p = const.), where p is a mean stress and q is a deviator stress, is adopted for the shear yield and the shear failure of clay in the modified Cam-clay model. The shear yield is caused by the increase in stress ratio $\eta = q/p$, while the compressive yield is caused by the increase in mean stress p. However, as the experimental evidence shows, the Extended Mises criterion grossly overestimates the strength in triaxial extension, and also results in incorrect intermediate stress ratios in plane strain[2]. In contrast with the Extended Mises failure, the SMP failure criterion[3], which is considered to be a three-dimensional extension of the Mohr-Coulomb criterion, is one of the failure criteria explaining well the recent test results of soils. A transformed stress tensor $\tilde{\sigma}_{ij}$ has been proposed by authors[4], which is deduced from what makes the SMP criterion become circular in the transformed π-plane. The transformed stress tensor $\tilde{\sigma}_{ij}$ is applied to the modified Cam-clay model in this paper. The revised model has realized the consistency from the shear yield to the shear failure of soils in three-dimensional stresses, both of which obey the SMP criterion, and the combination of the idea of critical state theory with the SMP criterion for clay.

On the other hand, the plastic volumetric strain ε_v^p is taken as its hardening parameter in the modified Cam-clay model, which is not appropriate for dilatant sand. So far, a lot of hardening parameters, which can describe the dilatancy of soils, have been assumed[5-9]. Several plasticity models have been proposed in the past[10-13]. The aim of this paper is to develop a simpler, practical and unified three-dimensional elastoplastic model for both clay and sand. For this reason, a new hardening parameter is derived on the basis of the consideration that the unified yield and plastic potential functions, which are the same as those of the modified Cam-clay model, are adopted for both clay and sand. The proposed hardening parameter is a revised plastic volumetric strain, the physical meaning of which is clear. This hardening parameter can not only describe the dilatancy from lightly to heavily dilatant sand, but also be reduced to the plastic volumetric strain ε_v^p for clay. The validity of the hardening parameter is confirmed by the test results of triaxial compression and extension tests on sand under the various stress paths.

Finally, the capability of the proposed model in predicting drained behavior of normally consolidated clay and saturated sand has been examined under triaxial compression and extension conditions. The results predicted by the proposed model agree well with the test results in triaxial compression and extension. Only five soil parameters are needed in the proposed model. The five soil parameters can be determined by a loading and unloading isotropic consolidation test and a conventional triaxial compression test. In this paper, the term stress is to be interpreted as effective stress.

* Received date: 2001-06-18

2 A transformed stress tensor based on SMP criterion

A transformed stress tensor $\tilde{\sigma}_{ij}$, by which the SMP criterion is drawn circular in the transformed π-plane, has been proposed by authors[4]. The outline of the transformed stress tensor $\tilde{\sigma}_{ij}$ will be reviewed as follows:

The SMP criterion is written as

$$\left.\begin{aligned}\frac{\tau_{\mathrm{SMP}}}{\sigma_{\mathrm{SMP}}} &= \sqrt{\frac{I_1 I_2 - 9I_3}{9I_3}} = \text{const.}\\ \text{or}\quad \frac{I_1 I_2}{I_3} &= \text{const.}\end{aligned}\right\} \tag{1}$$

where τ_{SMP} and σ_{SMP} are the shear and normal stresses on the SMP; and I_1, I_2 and I_3 are the first, second and third stress invariants.

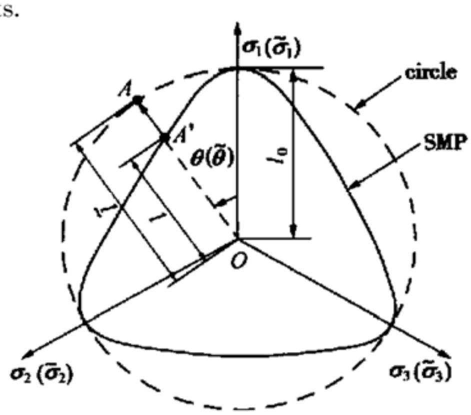

Fig. 1 SMP criterion in π-plane (solid curve) and transformed π-plane (broken circle)

In Fig. 1, the SMP criterion can be drawn by the solid line (a smoothly convex curve) in the ordinary π-plane, and the broken line (a circle) in the transformed π-plane (called $\tilde{\pi}$- plane for short). In the condition that the principal directions of $\tilde{\sigma}_{ij}$ and σ_{ij} are the same, as shown in Fig. 1, $\tilde{\sigma}_{ij}$ of point A, which corresponds to σ_{ij} of point A', can be obtained as follows[4]:

$$\tilde{\sigma}_{ij} = \tilde{p}\delta_{ij} + \tilde{s}_{ij} = p\delta_{ij} + \frac{l_0}{\sqrt{s_{kl}s_{kl}}}s_{ij} \tag{2}$$

where δ_{ij} is Kronecker's delta, $s_{ij}\,(=\sigma_{ij} - p\delta_{ij})$ deviatoric stress tensor in the ordinary stress space, and

$$\left.\begin{aligned}\tilde{p} &= \tilde{\sigma}_{ii}/3\\ \tilde{s}_{ij} &= \tilde{\sigma}_{ij} - \tilde{p}\delta_{ij}\end{aligned}\right\} \tag{3}$$

$$l_0 = \sqrt{\frac{2}{3}} \cdot \frac{2I_1}{\sqrt{(I_1 I_2 - I_3)/(I_1 I_2 - 9I_3)} - 1} \tag{4}$$

From the above derivation, it can be known that the shape of the SMP criterion becomes a cone with the axis being the space diagonal $\tilde{\sigma}_1 = \tilde{\sigma}_2 = \tilde{\sigma}_3$ in the transformed principal stress space, and becomes a circle with the center being the origin O in the $\tilde{\pi}$-plane (see Fig. 1). Taking the similarity in the shapes of the Extended Mises criterion in the principal stress space and the SMP criterion in the transformed principal stress space, into consideration, the existing elasto-plastic models, such as the Cam-clay model, can be revised easily with using the transformed stress tensor $\tilde{\sigma}_{ij}$.

Eq. (2) can also become

$$\left.\begin{aligned}\tilde{\sigma}_{ij} &= \frac{l_0}{\sqrt{s_{kl}s_{kl}}}\sigma_{ij} + \left(1 - \frac{l_0}{\sqrt{s_{kl}s_{kl}}}\right)p\delta_{ij}\\ \text{or}\quad&\\ \tilde{\sigma}_{ij} &= \left(\frac{l_0}{\sqrt{s_{kl}s_{kl}}}\delta_{im} + \left(1 - \frac{l_0}{\sqrt{s_{kl}s_{kl}}}\right)p\sigma^*_{im}\right)\sigma_{mj} = c_{im}\sigma_{mj}\end{aligned}\right\} \tag{5}$$

where c_{im} is a transformed tensor, which can be written as

$$c_{ij} = \frac{l_0}{\sqrt{s_{kl}s_{kl}}}\delta_{ij} + \left(1 - \frac{l_0}{\sqrt{s_{kl}s_{kl}}}\right)p\sigma^*_{ij} \tag{6}$$

where σ^*_{ij} is the inverse tensor of σ_{ij}, which can be written as

$$\left.\begin{aligned}\sigma^*_{ij} &= \frac{\Delta_{ji}}{\det\sigma}\\ \Delta_{ij} &= \frac{1}{2}e_{ipq}e_{jrs}\sigma_{pr}\sigma_{qs}\\ \det\sigma &= \frac{1}{6}e_{ijk}e_{rst}\sigma_{ir}\sigma_{js}\sigma_{kt}\end{aligned}\right\} \tag{7}$$

where e_{ijk} is Permutation symbol.

3 A unified hardening parameter for both clay and sand

The modified Cam-clay model is considered to be one of the best basic elasto-plastic models for clay, which is better than the original model[14]. In the modified Cam-clay model, the yield and plastic potential functions are assumed to be in the same form as follows:

$$f = g = \ln\frac{p}{p_0} + \ln\left(1 + \frac{q^2}{M^2 p^2}\right) - \int\frac{\mathrm{d}\varepsilon_v^p}{c_p} = 0 \tag{8}$$

where p_0 is the initial mean stress, M is the value of q/p at the critical state, $\mathrm{d}\varepsilon_v^p$ is the plastic volumetric strain increment, and c_p can be written as

$$c_p = \frac{\lambda - \kappa}{1 + e_0} \tag{9}$$

where λ is the compression index; κ is the swelling index; and e_0 is the initial void ratio at $p = p_0$.

It is possible that Eq. (8) is chosen as the plastic potential function of sand, because the dilatancy equation in modified Cam-clay model can also explain dilatant behavior of sand when $\eta > M$. The dilatancy equation is written as follows:

$$\frac{\mathrm{d}\varepsilon_v^p}{\mathrm{d}\varepsilon_d^p} = \frac{M^2 - \eta^2}{2\eta} \tag{10}$$

where $\mathrm{d}\varepsilon_d^p$ is the plastic deviator strain increment. From Eq. (10), it can be see that when $0 < \eta < M$, $\mathrm{d}\varepsilon_v^p > 0$ (negative dilatancy condition), and when $M < \eta \leqslant M_f$, $\mathrm{d}\varepsilon_v^p < 0$ (positive dilatancy condition), in which M is the phase transformation stress ratio and M_f the peak stress ratio. In order to adopt the associated flow rule, the yield function similar to Eq. (8) is also assumed for sand. However, the plastic volumetric strain cannot be used as the hardening parameter (see the test results of the next section in detail). A new hardening parameter H is derived to describe the hardening behavior of both clay and sand as follows. The yield and plastic potential functions for sand are written as

$$f = g = \ln\frac{p}{p_0} + \ln\left|1 + \frac{q^2}{M^2 p^2}\right| - H = 0 \quad (11)$$

The hardening parameter is usually considered to be a combination of the plastic strain increment tensor $d\varepsilon_{ij}^{p}$[7], e.g., the plastic work type hardening parameter. Thus, the following hardening parameter is assumed:

$$H = \int dH = \int \left| c_1(\sigma_{ij}) d\varepsilon_v^p + c_2(\sigma_{ij}) d\varepsilon_d^p \right| \quad (12)$$

where $c_1(\sigma_{ij})$ and $c_2(\sigma_{ij})$ are all the functions of the stress tensor. Substituting Eq.(10) into (12) gives

$$H = \int \left| c_1(\sigma_{ij}) d\varepsilon_v^p + c_2(\sigma_{ij}) \frac{2\eta}{M^2 - \eta^2} d\varepsilon_v^p \right| = \int c(\sigma_{ij}) d\varepsilon_v^p \quad (13)$$

where $c(\sigma_{ij})$ is the function of the stress tensor. Fig. 2 shows the constant mean stress path (path AB) and the isotropic compression stress path (path AC) along which the hardening parameter changes from H_0 to H. The process of the derivation, by which the hardening parameter H is developed, i.e., $c(\sigma_{ij})$ in Eq.(13) is determined, is ①to derive the concrete equation of H along path AB; and ②to make this equation be consistently tenable along path AC since the hardening parameter H in the same yield should be the same.

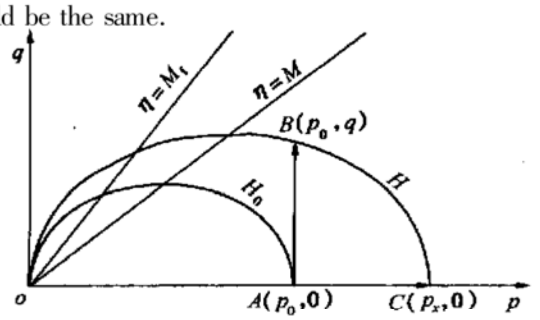

Fig. 2 Stress paths on deriving hardening parameter H

3.1 Along constant mean stress path

After substituting Eq.(13) to Eq.(11), the proportionality constant Λ can be written as

$$\Lambda = \frac{1}{c(\sigma_{ij})} \frac{\frac{\partial f}{\partial p}dp + \frac{\partial f}{\partial q}dq}{\frac{\partial f}{\partial p}} \quad (14)$$

Based on Eq.(11), the following two differential equations can be obtained:

$$\left.\begin{aligned} \frac{\partial f}{\partial p} &= \frac{1}{p} \cdot \frac{M^2 - \eta^2}{M^2 + \eta^2} \\ \frac{\partial f}{\partial q} &= \frac{1}{p} \cdot \frac{2\eta}{M^2 + \eta^2} \end{aligned}\right| \quad (15)$$

By substituting Eq.(15) into Eq.(14), the plastic deviator strain increment can be expressed as follows along the constant mean stress path:

$$d\varepsilon_d^p = \Lambda \frac{\partial f}{\partial q} = \frac{1}{c(\sigma_{ij})} \cdot \frac{1}{p} \cdot \frac{4\eta^2}{M^4 - \eta^4} dq \quad (16)$$

Fig. 3 shows the triaxial compression test results of clay and sand arranged in (a) $\eta - \varepsilon_d$ and (b) $\frac{M_f^4 - \eta^4}{4\eta^2} - \frac{d\eta}{d\varepsilon_d}$ (data from references[15, 16]). It can be seen from Fig. 3 (a) that the shapes of the curves for clay and sand are alike. The stress ratios (q/p) at failure for clay and sand are M and M_f respectively. In fact, M_f is not constant during shearing. If the variety of M_f is considered during shearing, more complex behavior (e.g., the softening) of soils can be described[17]. In this paper, M_f is simply assumed as a constant to focus attention on explaining the behavior due to the proposed hardening parameter. Therefore, compared with the equation of the plastic deviator strain increment for clay in the modified Cam-clay model when the mean stress is constant, the equation of the plastic deviator strain increment for sand is assumed to be Eq.(17) when the mean stress is constant.

$$\left.\begin{aligned} d\varepsilon_d^p &= c_p \cdot \frac{1}{p} \cdot \frac{4\eta^2}{M^4 - \eta^4} dq \quad \text{(clay)} \\ d\varepsilon_d^p &= \rho \cdot \frac{1}{p} \cdot \frac{4\eta^2}{M_f^4 - \eta^4} dq \quad \text{(sand)} \end{aligned}\right| \quad (17)$$

where ρ is a constant. On the other hand, Eq.(17) can also become the following linear forms respectively:

$$\left.\begin{aligned} \frac{M^4 - \eta^4}{4\eta^2} &= c_p \frac{d\eta}{d\varepsilon_d^p} \quad \text{(clay)} \\ \frac{M_f^4 - \eta^4}{4\eta^2} &= \rho \frac{d\eta}{d\varepsilon_d^p} \quad \text{(sand)} \end{aligned}\right| \quad (18)$$

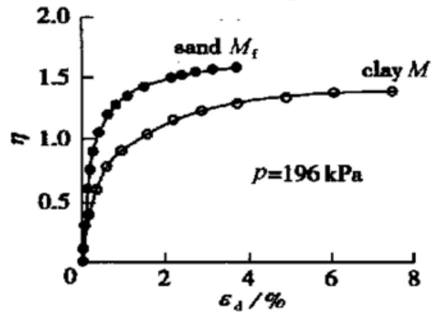

(a) $\eta - \varepsilon_d$

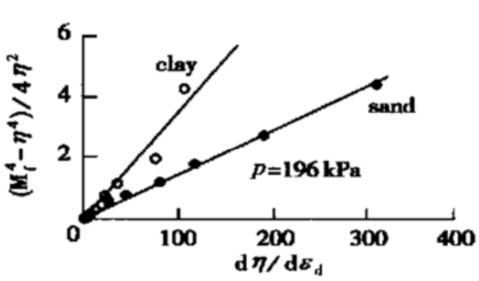

(b) $\frac{M_f^4 - \eta^4}{4\eta^2} - \frac{d\eta}{d\varepsilon_d}$

Fig. 3 Triaxial compression test results for clay and sand

The validity of Eq.(18) is confirmed by the test results of triaxial compression from Fig. 3(b). So, Eq.(17) is also rational for sand. It is worth noting that $M_f = M$ for clay and the elastic deviator strain is very small under a constant mean stress in Fig. 3(b). By combining Eq.(16) and (17), $c(\sigma_{ij})$ in Eqs.(16) is expressed as

$$c(\sigma_{ij}) = \frac{1}{\rho} \cdot \frac{M_f^4 - \eta^4}{M^4 - \eta^4} \tag{19}$$

Substituting Eq. (19) into Eq. (13) gives

$$H = \int dH = \int \frac{1}{\rho} \cdot \frac{M_f^4 - \eta^4}{M^4 - \eta^4} d\varepsilon_v^p \tag{20}$$

3.2 Along isotropic compression stress path

When $\eta = 0$ (path AC), Eq. (20) becomes

$$H = \int dH = \int \frac{1}{\rho} \cdot \frac{M_f^4}{M^4} d\varepsilon_v^p \tag{21}$$

Moreover, under the isotropic compression condition ($\eta = \frac{q}{p} = 0$), $\int \frac{d\varepsilon_v^p}{c_p} = \ln(\frac{p}{p_0})$ in Eq. (8). Eq. (11) becomes $\int dH = \ln(\frac{p}{p_0})$ when $\eta = 0$. So, the following equation can be obtained.

$$H = \int dH = \int \frac{d\varepsilon_v^p}{c_p} \tag{22}$$

Letting Eq. (21) be equal to Eq. (22) obtains

$$\rho = c_p \cdot \frac{M_f^4}{M^4} \tag{23}$$

Finally, the new hardening parameter for sand can be obtained by substituting Eq. (23) into Eq. (20)

$$H = \int dH = \int \frac{1}{c_p} \cdot \frac{M^4}{M_f^4} \cdot \frac{M_f^4 - \eta^4}{M^4 - \eta^4} d\varepsilon_v^p \tag{24}$$

If $M = M_f$, Eq. (24) becomes $H = \int dH = \int \frac{d\varepsilon_v^p}{c_p}$, which is the same as the hardening parameter for clay in the modified Cam-clay model. Therefore, the new hardening parameter (Eq. (24)) is a unified one for both clay and sand.

How the proposed model describes the dilatancy of soil is explained as follows. From Eq. (24) and considering 3-D stress conditions, get

$$d\varepsilon_v^p = c_p \cdot \frac{M_f^4}{M^4} \cdot \frac{M^4 - \tilde{\eta}^4}{M_f^4 - \tilde{\eta}^4} d\tilde{H} \tag{25}$$

Taking that $d\tilde{H}$ is always larger than or equal to 0 into account, the following conclusions can be obtained from Eq. (25): ① $\tilde{\eta} = 0$ (isotropic consolidation condition), $d\varepsilon_v^p = c_p d\tilde{H}$; ② $0 \leqslant \tilde{\eta} < M$ (negative dilatancy condition), $d\varepsilon_v^p > 0$; ③ $\tilde{\eta} = M$ (phase transformation condition[18, 19]), $d\varepsilon_v^p = 0$; ④ $M < \tilde{\eta} \leqslant M_f$ (positive dilatancy condition), $d\varepsilon_v^p < 0$.

As indicated above, the dilatancy of sand is reasonably described by using the new hardening parameter $\tilde{H}$. The validity of $\tilde{H}$ and the other usual state quantities used as hardening parameters will be checked in the various stress paths as follows.

Fig. 4 shows the stress paths in triaxial tests on Toyoura sand (data from reference[16]) in terms of the relation between mean stress p and deviator stress q. The values of the principal stress ratios are the same ($\sigma_1/\sigma_3 = 4$) at points F and F' in Fig. 4. The stress path dependency of four state quantities, the plastic volumetric strain ε_v^p, the plastic deviator strain ε_d^p, the plastic work W^p and the proposed hardening parameter $\tilde{H}$, will be checked in four kinds of triaxial compression tests (paths: $ADEF$, $ABCF$, AF and $ABEF$) and three kinds of triaxial extension tests (paths: $AD'F'$, ACF' and AF'). Figs. 5 to 8 show the variations of these quantities along the seven kinds of stress paths under triaxial compression and extension conditions. It is obvious from Figs. 5 to 7 that the plastic volumetric strain ε_v^p, the plastic deviator strain ε_d^p and the plastic work W^p are unsuitable for the hardening parameter for sand, because these state quantities depend on the stress paths at the same stress state. However, Fig. 8 shows that the values of the proposed hardening parameter $\tilde{H}$ are uniquely determined at the same stress state, regardless of the stress-path in triaxial compression and extension and the previous stress history. So, $\tilde{H}$ is employed as a new hardening parameter for sand.

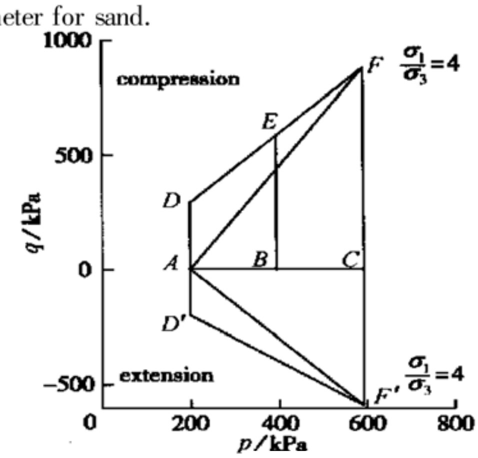

Fig. 4 Stress paths of triaxial tests for examining new hardening parameter

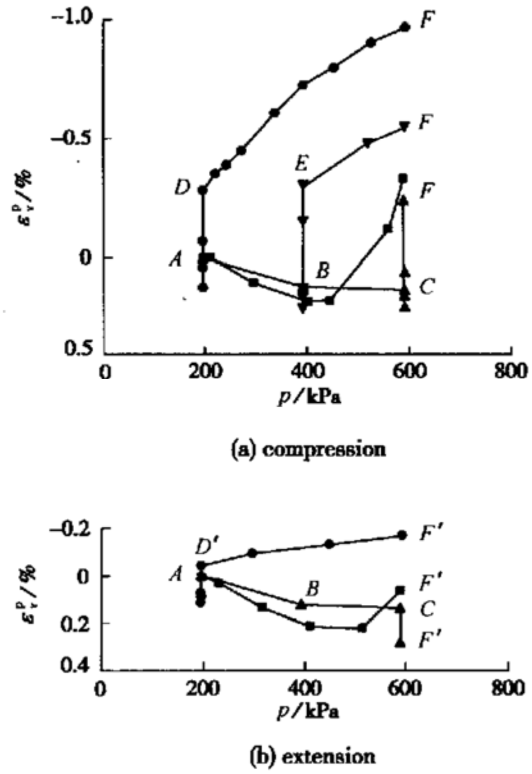

Fig. 5 Relation between plastic volumetric strain ε_v^p and mean principal stress p

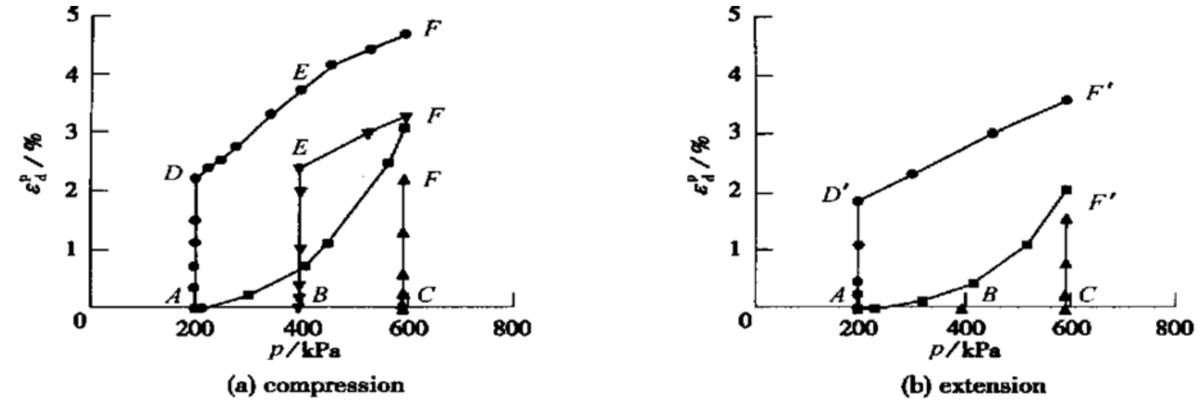

Fig. 6 Relation between plastic deviatoric strain ε_d^p and mean principal stress p

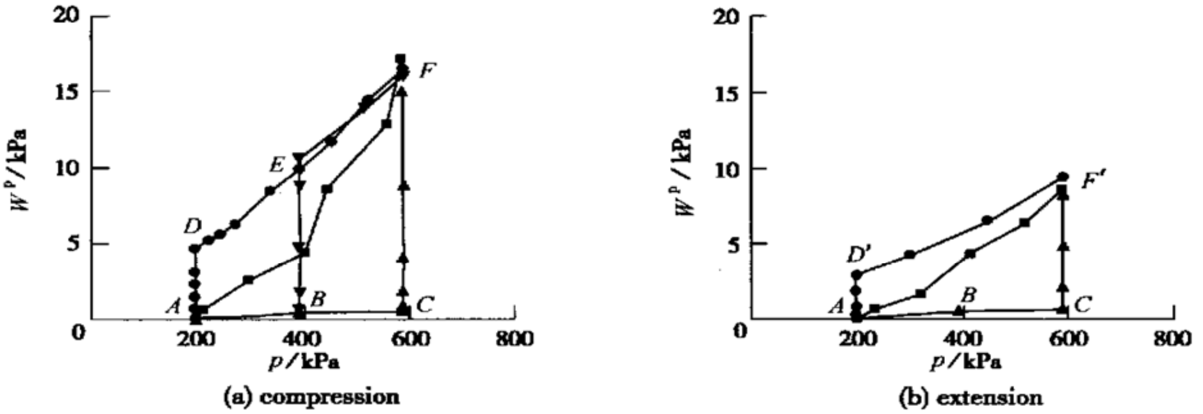

Fig. 7 Relation between plastic work W^p and mean principal stress p

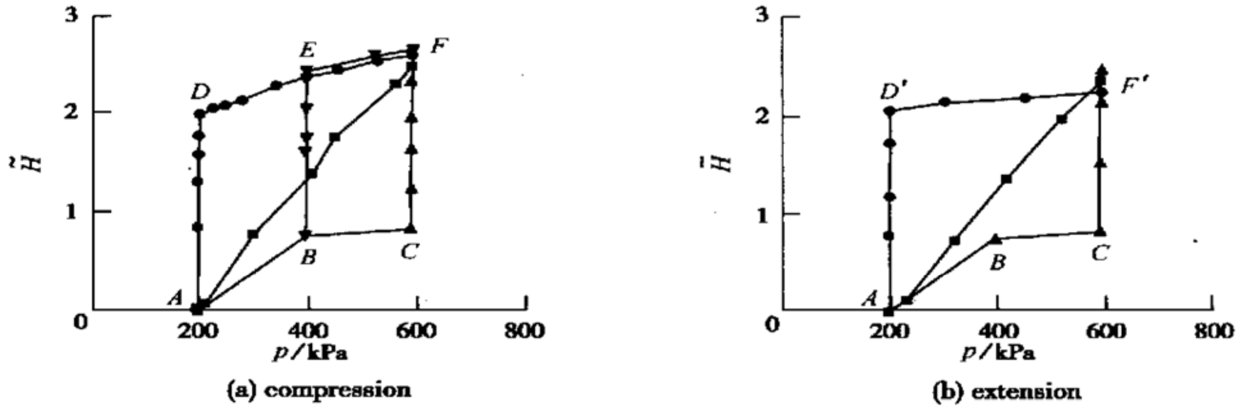

Fig. 8 Relation between new hardening parameter $\widetilde{H}$ and mean principal stress p

4 A unified elasto-plastic model for both clay and sand

In the proposed model, the equations of the yield locus and plastic potential remain the same as the modified Cam-clay model's, but the transformed stress tensor $\tilde{\sigma}_{ij}$ based on the SMP and the new hardening parameter are adopted to model the behavior of clay and sand in three-dimensional stresses.

The plastic component is given by assuming the flow rule not in σ_{ij} space but in $\tilde{\sigma}_{ij}$ space.

$$d\varepsilon_{ij}^p = \Lambda \frac{\partial g}{\partial \tilde{\sigma}_{ij}} \tag{26}$$

where the plastic potential function g (or the yield function f), the hardening parameter $\widetilde{H}$, the proportionality constant Λ and the differential equation $\frac{\partial g}{\partial \tilde{\sigma}_{ij}}$ are given respectively as follows:

$$\left.\begin{aligned}
f = g = \ln\frac{\tilde{p}}{\tilde{p}_0} + \ln\left(1 + \frac{\tilde{q}^2}{M^2\tilde{p}^2}\right) - \widetilde{H} = 0 \\
\widetilde{H} = \int d\widetilde{H} = \int \frac{1}{c_p}\cdot\frac{M^4}{M_f^4}\cdot\frac{M_f^4 - \tilde{\eta}^4}{M^4 - \tilde{\eta}^4} d\varepsilon_v^p \\
\Lambda = c_p \cdot \frac{M_f^4}{M^4}\cdot\frac{M^4 - \tilde{\eta}^4}{M_f^4 - \tilde{\eta}^4}\left(d\tilde{p} + \frac{2\tilde{p}\tilde{q}}{M^2\tilde{p}^2 - \tilde{q}^2} d\tilde{q}\right) \\
\frac{\partial g}{\partial \tilde{\sigma}_{ij}} = \frac{1}{M^2\tilde{p}^2 + \tilde{q}^2}\left(\frac{M^2\tilde{p}^2 - \tilde{q}^2}{3\tilde{p}}\delta_{ij} + 3(\tilde{\sigma}_{ij} - \tilde{p}\delta_{ij})\right)
\end{aligned}\right\} \tag{27}$$

where the deviator stress $\tilde{q}$ and the transformed stress ratio $\tilde{\eta}$ in $\tilde{\sigma}_{ij}$ space, M ($\tilde{\eta}$ at phase transformation) and M_f ($\tilde{\eta}$ at peak) are written respectively as follows:

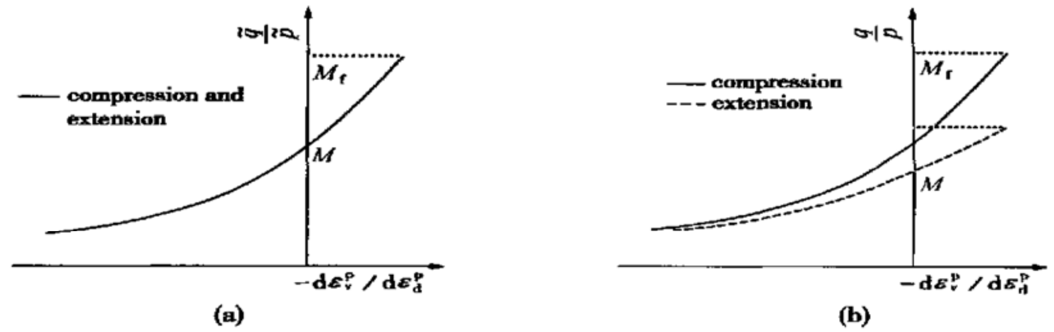

Fig. 9 Stress-dilatancy relationships of proposed model under triaxial compression and extension conditions

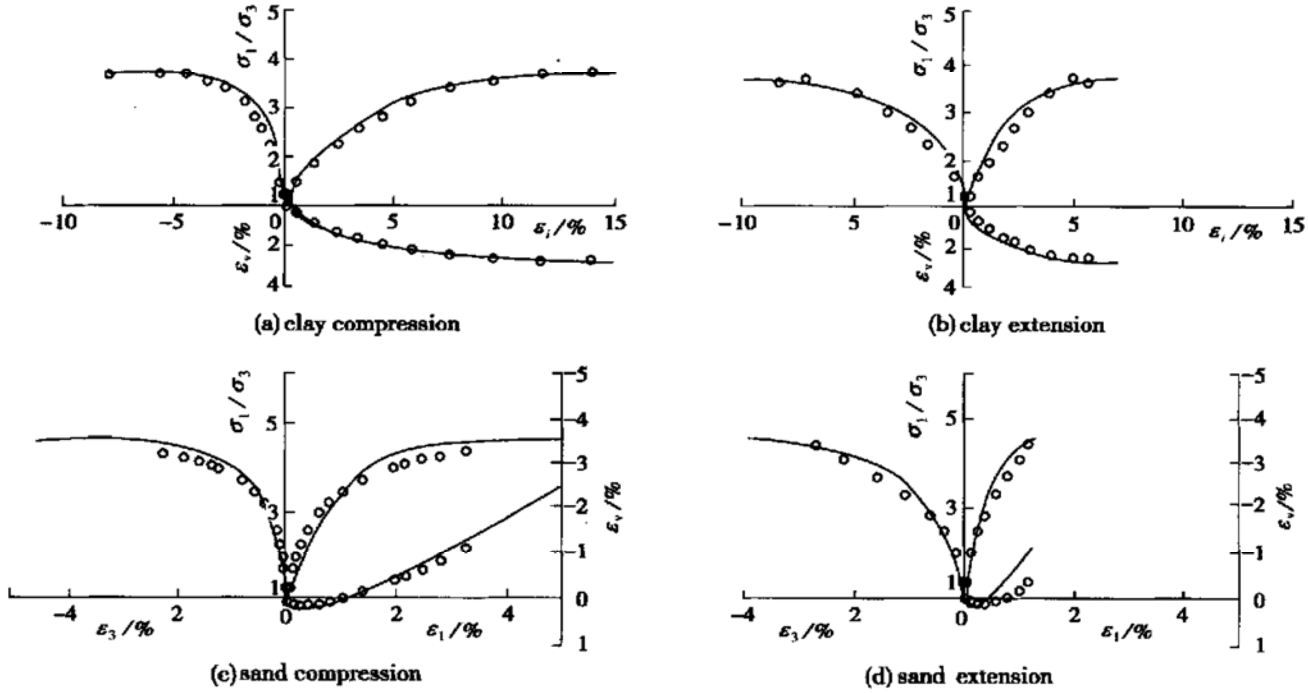

Fig. 10 Comparison between predicted and test results when p = 196 kPa for clay and sand

$$\left.\begin{aligned} \tilde{\eta} &= \tilde{p}/\tilde{q} \\ \tilde{q} &= \sqrt{\frac{3}{2}\tilde{s}_{ij}\tilde{s}_{ij}} \\ M &= \frac{6\sin\varphi_{pt}}{(3-\sin\varphi_{pt})} \\ M_f &= \frac{6\sin\varphi}{(3-\sin\varphi)} \end{aligned}\right\} \tag{28}$$

where $\tilde{p}_0(=p_0)$ is the initial mean stress: φ_{pt} is the angle of internal friction at the phase transformation; and φ is the angle of internal friction at the shear failure. The main features of the proposed model for both clay and sand will be presented as follows.

4.1 For sand

The stress-dilatancy equation of the proposed model is expressed as follows:

$$\frac{d\varepsilon_v^p}{d\varepsilon_d^p} = \frac{M^2\tilde{p}^2 - \tilde{q}^2}{2\tilde{p}\tilde{q}} \tag{29}$$

Eq. (29) can be drawn as Fig. 9(a) in the $\frac{\tilde{q}}{\tilde{p}}$ – $\left|-\frac{d\varepsilon_v^p}{d\varepsilon_d^p}\right|$ plane and as Fig. 9(b) in the $\frac{q}{p}$ – $\left|-\frac{d\varepsilon_v^p}{d\varepsilon_d^p}\right|$ plane under triaxial compression and extension conditions. It is seen form these two figures that the unique relationship between $\frac{\tilde{q}}{\tilde{p}}$ and $-\frac{d\varepsilon_v^p}{d\varepsilon_d^p}$ (See Fig. 9(a)) can explain the different in relation (See Fig. 9(b)) between triaxial compression and extension.

4.2 For clay

As mentioned before, If $M = M_f$, the new hardening parameter $\tilde{H}$ in the proposed model becomes the plastic volumetric strain, which is the same as the hardening parameter for clay in the modified Cam-clay model. Therefore, the difference between the proposed model and the modified Cam-clay model is only the stress tensor used. The critical state conditions of the proposed model in three-dimensional stresses can be expressed as follows:

$$\left.\begin{aligned} \tilde{\eta}_{cs} &= \frac{\tilde{q}_{cs}}{\tilde{p}_{cs}} = M \\ \frac{d\varepsilon_v^p}{d\varepsilon_d^p} &= 0 \\ \varepsilon_v^p &= c_p\left|\ln\frac{\tilde{p}_{cs}}{\tilde{p}_0} + \ln 2\right| \\ \varepsilon_d^p &\to \infty \end{aligned}\right\} \tag{30}$$

where suffix cs means the critical state. When Eq. (30) is satisfied, soil will be continuously distorted. Eq. (30) is the same as the critical state conditions of the modified Cam-clay model in triaxial compression, so it is the extension form for the critical state conditions of the modified Cam-clay model in three-dimensional stresses.

5 Prediction versus experiment

The capability of the proposed model in predicting drained behavior of clay and sand has been examined in p = 196 kPa, not only under triaxial compression, but also under triaxial extension on normally consolidated Fujinomori clay and saturated Toyoura sand[15, 16]. The values of soil parameters used in the model are $M = M_f = 1.45$, $\frac{\lambda}{1+e_0} = 0.0508$, $\frac{\kappa}{1+e_0} = 0.0112$ and $\nu = 0.3$ for Fujinomori clay, and $M = 0.95$, $M_f = 1.66$, $\frac{\lambda}{1+e_0} = 0.00403$, $\frac{\kappa}{1+e_0} = 0.00251$ and $\nu = 0.3$ for Toyoura sand respectively. The above soil parameters are determined by the isotropic consolidation test and the conventional compression tests. Fig. 10 shows the predicted and test results on the drained behavior of Fujinomori clay and Toyoura sand under triaxial compression and extension conditions when p = 196 kPa. It can be seen from Fig. 10 that the results (solid lines) predicted by the proposed model agree well with the test results (mark ○) for clay and sand under triaxial compression and extension conditions.

Therefore, it can be seen from the above comparison that the proposed model can reasonably describe the stress-strain characteristics of clay and sand in three-dimensional stresses, and the dilatancy of sand.

6 Conclusions

(1) A new hardening parameter is derived on the basis of the consideration that the simpler, unified yield and plastic potential functions are adopted for both clay and sand. It can not only describe the dilatancy from lightly to heavily dilatant sand, but also be reduced to the plastic volumetric strain for clay. The validity of hardening parameter $\widetilde{H}$ is confirmed by the test results of triaxial compression and extension tests on sand under the various stress paths.

(2) An elasto-plastic model is proposed by applying the transformed stress tensor $\tilde{\sigma}_{ij}$ based on the SMP and the new hardening parameter $\widetilde{H}$ to the modified Cam-clay model. The proposed model can reasonably describe the stress-strain behavior of clay and sand in three-dimensional stresses.

(3) Five soil parameters (λ, κ, φ_{pt}, φ and ν) in the proposed model can be determined by an isotropic consolidation test and a conventional triaxial compression test.

References

[1] Roscoe K H, Burland J B. On the generalized stress-strain behavior of ‘wet’ clay[A]. Heyman J, Leckie F A. Engineering Plasticity [C]. Cambridge: Cambridge University Press, 1968. 535- 609.

[2] Wroth C P, Houlsby G T. Soil mechanics-property characterization and analysis procedures[A]. Proceedings of the 11th International Conference on Soil Mechanics and Foundations Engineering[C]. San Francisco, 1985. 1- 55.

[3] Matsuoka H, Nakai T. Stress-deformation and strength characteristics of soil under three difference principal stresses[J]. JSCE Journal, 1974, **232**: 59- 70.

[4] Matsuoka H, Yao Y P, Sun D A. The Cam-clay models revised by the SMP criterion[J]. Soils and Foundations, 1999, **39**(1): 81- 95.

[5] Lade P V. Elasto-plastic stress-strain theory for cohesionless soils curved yield surface[J]. International Journal of Solids and Structures, 1977, **13**: 1019- 1035.

[6] Nova R, Wood D M. A constitutive model for sand in triaxial compression[J]. International Journal for Numerical and Analytical Methods in Geomechanics, 1979, **3**: 225- 278.

[7] Huang W X, Pu J L, Chen Y J. Hardening rule and yield function for soils[A]. Proceedings of the 10th International Conference on Soil Mechanics and Foundations Engineering[C]. 1981. 631- 634.

[8] Bardet J P. Bounding surface model for sands[J]. Journal of Engineering Mechanics, ASCE, 1986, **112**(11): 1198- 1217.

[9] Lade P V, Prabucki M J. Softening and preshearing effects in sand[J]. Soils and Foundations, 1995, **35**(4): 95- 104.

[10] Hashiguchi K, Ueno M. Elasto-plastic constitutive laws of granular materials[A]. Proceedings of Special Session 9 of 9th International Conference on Soil Mechanics and Foundations Engineering[C]. Tokyo: JSSMFE, 1977. 73- 82.

[11] Prevost J H. A simple plasticity theory for frictional cohesionless soils[J]. Soil Dynamics and Earthquake Engineering, 1985, **4** (1): 9- 17.

[12] Zienkiewicz O C, Leung K H, Pastor M. A simple model for transient loading in earthquake analysis (part Ⅰ): basic model [J]. International Journal for Numerical and Analytical Methods in Geomechanics, 1985, **9**: 453- 476.

[13] Dafalias Y F. Bounding surface plasticity Ⅰ: theory[J]. Journal of Engineering Mechanics, ASCE, 1986, **112**(12): 1242- 1291.

[14] Roscoe K H, Schofield A N, Thurairajah A. Yielding of clay in states wetter than critical[J]. Geotechnique, 1963, **13**(3): 211 - 240.

[15] Nakai T, Matsuoka H. A generalized elastoplastic constitutive model for clay in three-dimensional stresses[J]. Soils and Foundations, 1986, **26**(3): 81- 98.

[16] Nakai T. An isotropic hardening elastoplastic model considering the stress path dependency in three-dimensional stresses[J]. Soils and Foundations, 1989, **29**(1): 119- 139.

[17] Yao Y P, Matsuoka H, Sun D A. A unified elastoplastic model of sand dependent on stress level and void ratio[A]. Proceedings of 2nd International Symposium on Prefailure Deformation Characteristics of Geomaterials[C]. Rotterdam: Balkema, 1999. 589- 596.

[18] Ishihara K. Liquefaction and flow failure during earthquakes (Thirty-third Rankine Lecture)[J]. Geotechnique, 1993, **43**(3): 351- 415.

[19] Ishihara K, Tatsuoka F, Yasuda S. Undrained deformation and liquefaction of sand under cyclic stresses[J]. Soils and Foundations, 1975, **15**(1): 29- 44.